Spectral Sensitization of n-Type TiO_2 Electrodes by Polypyridineruthenium(II) Complexes

W. D. K. Clark and N. Sutin*

Contribution from the Chemistry Department, Brookhaven National Laboratory, Upton, New York 11973. *Received January 7, 1977*

Abstract: The spectral sensitization of single-crystal n-type TiO_2 electrodes by polypyridineruthenium(II) complexes has been studied as a function of the pH of the solution. The results show that the energy of the conduction band edge of TiO_2 must be higher than the value estimated on the basis of current models. Evidence for the existence of an intermediate level in n-type TiO_2 in aqueous media is presented. The quantum yield for electron injection by the excited state of tris(4,7-dimethyl-1,10-phenanthroline)ruthenium(II) is close to unity. The implication of the results for a solar energy conversion system is discussed.

Spectral sensitization of wide band-gap semiconductor electrodes has been described by a number of workers.[1-3] In this process charge carriers are produced in the semiconductor as a consequence of the excitation of electrons in dyes adsorbed on the semiconductor surface. Studies of this phenomenon have shown that electron transfer can occur either to (anodic photocurrent) or from (cathodic photocurrent) the semiconductor depending upon the relative positions of the energy levels in the semiconductor and the excited dye (Figure 1).[4]

A recent report has shown that excitation of tris(2,2′-bipyridine)ruthenium(II) [$Ru(bpy)_3^{2+}$] gives rise to anodic photocurrents at a SnO_2 electrode.[5] This is not unexpected since electron transfer from the excited state of the complex to the conduction band of the semiconductor is favored by about 1 eV.[6] More quantitative information on the factors governing such charge-transfer processes can be gathered by examining systems for which the energy levels of the sensitizer and of the electrode can be varied in a systematic manner. Such a situation should obtain for a series of ruthenium complexes and a TiO_2 electrode in an aqueous medium.

Ruthenium complexes of organic ligands such as bipyridine and phenanthroline have been well characterized spectrally and electrochemically.[7] The reduction potentials of these complexes vary with the nature of the ligands and are relatively independent of pH. The absorption and emission spectra vary little from compound to compound or with the medium. Therefore, the energies of the excited states of the complexes can be located quite accurately on the electrochemical scale[8] for this work.

TiO_2 (rutile) was chosen for this study because of its flat-band potential,[9] wide band gap[9] (>3.0 eV as compared to the 2.7-eV absorption maximum of the ruthenium complexes), and chemical stability over a wide pH range.[10,11] In common with other oxide semiconductors, the energies of the conduction and valence bands of the TiO_2 electrode increase with increasing pH of the solution.[12] Therefore it is possible to independently change the energy levels of the electrode (by changing the pH) and those of the redox couple (by changing the nature of the complex) so as to go from a sensitizing to a nonsensitizing condition. Because of the relatively high dielectric constant of TiO_2[13] electron tunneling is likely to be much less important in this semiconductor than, for example, in SnO_2.[14] The absence of tunneling contributions should simplify the interpretation of the results. Finally, TiO_2 has been the subject of much investigation in connection with photographic processes and solar energy conversion.[10,15] The possibility of sensitizing TiO_2 to longer wavelengths is therefore of considerable interest and the use of polypyridineruthenium(II) complexes to effect this is of particular significance since these complexes have recently received attention as systems capable of photodecomposing water.[16]

Experimental Section

Materials. Sections of a TiO_2 crystal (Gallard-Schlesinger Atomergic Co.) were cut parallel to the 001 face. These 1-cm diameter, 1-mm thick slices were polished using successively finer materials in the order 320 mesh carborundum powder, 800 mesh carborundum powder, and 1 μm alumina. The samples were reduced in H_2 at 600 °C for periods of 0.5 to 2 h and cut to a final size of 0.1-cm^2 area. Indium solder was applied to the back of this chip; the solder provided both the ohmic contact and a means of attaching a copper wire. The electrode was mounted on the end of a glass tube in silicone rubber (Dow Corning) and treated with a mixture of hydrofluoric, nitric, and acetic acids[17a] for 15 s prior to use.

The ruthenium(II) complexes used in this work and their properties are listed in Table I. $Ru(bpy)_3Cl_2$ was obtained from G. F. Smith and purified as previously described.[7] Tris(5-chloro-1,10-phenanthroline)ruthenium(II) chloride, $Ru[5\text{-}Cl(phen)]_3Cl_2$, and tris(4,7-dimethyl-1,10-phenanthroline)ruthenium(II) chloride, $Ru[4,7\text{-}(CH_3)_2phen]_3Cl_2$, were prepared by standard procedures.[7] Acetonitrile (Matheson Coleman and Bell) was passed through a column of activated alumina prior to use.[17b] Water was triply distilled from acid dichromate, alkaline permanganate, and redistilled. Tetra-*n*-butylammonium perchlorate (Eastman) was purified by recrystallization from methanol. All other chemicals were standard reagent grade and were used without further treatment.

Apparatus and Procedure. Photocurrent measurements were made with the following apparatus. Light from a 450 W xenon lamp (Christie Electric Corp.) was passed through a Bausch and Lomb high-intensity monochromator and reflected up through the bottom of the electrochemical cell onto the TiO_2 electrode. For most of the measurements the monochromator was replaced by a set of Corning filters (5031 and 3389) which transmitted light between 520 and 420 nm (maximum at 470 nm). Band-gap excitation of TiO_2 was performed with the 5031 filter alone (390- to 520-nm transmittance). Before entering the cell the light beam was chopped at 27.2 Hz with a Princeton Applied Research Corp. (PAR) Model 125A light chopper. The signal from the chopper was fed to the reference channel of a PAR Model 124 lock-in amplifier. The cell was flushed with argon which had been passed over a hydrogen-reduced copper-based catalyst (type R3-11 from Chemical Dynamics Corp.) at 120 °C.

The TiO_2 electrode was the working electrode in a three-electrode configuration; the counter and reference electrodes were a cylinder of platinum gauze and a saturated calomel electrode (SCE), respectively. Contact between the solution and the SCE was made by means of a Luggin capillary (Figure 2). A waveform generator (PAR Model 175 universal programmer) was used to control the rate and range of the potential sweep of the potentiostat (PAR Model 173). Dark currents were measured with a PAR Model 179 coulometer. Photocurrents were determined by measuring the voltage drop across a 10 Ω resistor in series with the working electrode (Figure 3). This voltage drop was measured by a PAR Model 116 differential preamplifier which plugged into the signal channel of the lock-in amplifier. The dark current-potential and photocurrent-potential curves were plotted on a Hewlett Packard Model 7000 X-Y recorder.

The capacitance of the space-charge layer of the semiconductor was determined by superimposing a 1-mV sinusoidal voltage of 5-500

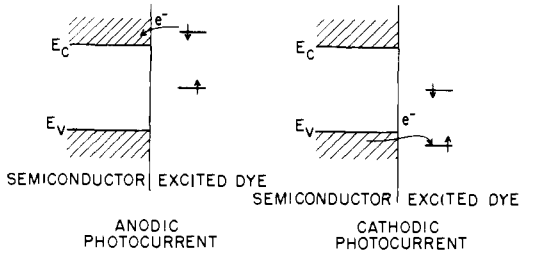

Figure 1. Relative positions of the energies of the bottom of the conduction band (E_c) and the top of the valence band (E_v) of a semiconductor electrode and those of a dye molecule in solution for anodic and cathodic photocurrents.

Table I. Spectral and Electrochemical Data for the Polypyridineruthenium(II) Complexes

	Absorption λ_{max}, nm	Emission λ_{max}, nm	V^0_{Ru} (V vs. SCE)	$^*V^0_{Ru}$ (V vs. SCE)
$Ru[5\text{-}Cl(phen)]_3Cl_2$	447	605	1.12	−1.01
$Ru(bpy)_3Cl_2$	452	613	1.02	−1.08
$Ru[4,7\text{-}(CH_3)_2phen]_3Cl_2$	445	612	0.85	−1.25

Hz from the reference channel of the lock-in amplifier onto the dc bias of the waveform generator. The 90° (capacitive) component of the resultant sinusoidal current was determined from the voltage drop across the 10 ohm resistor as measured by the lock-in amplifier. The system was calibrated by replacing the electrochemical cell by a standardized capacitor with capacitance approximately equal to that of the space-charge layer of the semiconductor.

A correction for ohmic losses was necessary for the acetonitrile solutions and/or the less conductive TiO_2 samples. This was accomplished by feeding a portion of the output from the current-voltage converter of the coulometer to the input of the potentiostat.[18] This feedback increased the measured current to a level that would have been obtained if no IR loss had occurred. The amount of IR compensation necessary was determined from the response of current-time curves to a small (1-20 mV) square-wave voltage (10^2-10^3 Hz) superimposed on the bias from the waveform generator. The current-time curves were monitored on an oscilloscope (Tektronix Model 585 with a type 82 plug-in).

The amount of IR compensation required was also determined by monitoring the 0° (resistive) component of the current. This component maximized when the proper amount of compensation was achieved; too much IR compensation caused the system to go into voltage and current oscillations. The IR compensation determined by the two methods was in good agreement.

The lack of proper IR compensation affected the capacitance and photocurrent measurements the most. The capacitive current becomes more sensitive to the IR compensation as the flat-band potential (V_{fb}) of the system was approached. It was found that as V approached V_{fb} more IR compensation was needed in order to maximize the 0° (resistive) component of the current. This gave a value for V_{fb} from the Mott-Schottky plots that agreed fairly well with literature values and with the potentials for the onset of the band-gap photocurrent. Therefore the capacitive current-potential curve was determined point by point and the compensation adjusted for each point.

Samples that required no IR compensation exhibited photocurrents (produced by light of band-gap or greater energy) that followed the square-wave form of the incident light. Under these conditions the maximum photocurrent measured by the lock-in amplifier was found to occur at a phase angle of 0° with respect to the chopped light. However, in samples requiring IR compensation, the photocurrent lagged behind the light pulse. This effect could be so severe that the photocurrent reached only a small fraction of its maximum value and its phase angle shifted many degrees. Application of the proper amount of IR compensation increased the photocurrent dramatically and returned the phase angle to 0°. In cases where IR compensation could not be adequately applied (very low doping levels), the band-gap photocurrent was measured by using an unchopped light beam.

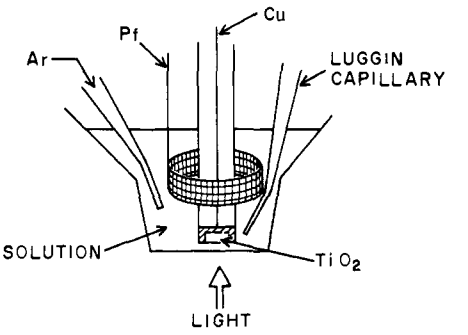

Figure 2. Diagram of the electrochemical cell and the electrode arrangement.

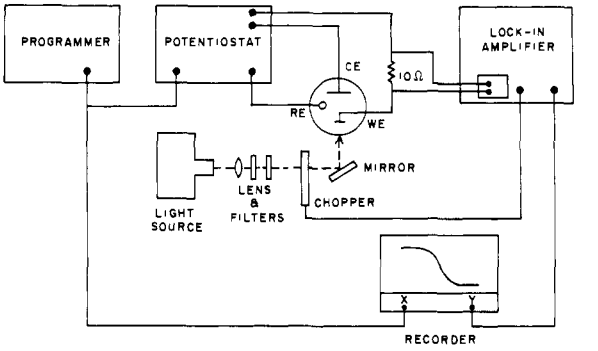

Figure 3. Schematic representation of the experimental arrangement: WE is the working electrode (TiO_2); RE is the reference electrode (SCE), and CE is the counter electrode (Pt).

For small photocurrents (<1 $\mu A/cm^2$), IR compensation could usually be done without any complications. However, with large photocurrents the difference between the light and dark portions of the chopped cycle caused large voltage shifts in the less conductive TiO_2 samples and oscillations of voltage occurred which were amplified when the IR compensation was applied. However, for these larger photocurrents, a measurement with continuous illumination could be made and the chopped light excitation was not necessary.

A typical experiment was carried out as follows: the components of the photoelectrochemical cell were assembled, and an aqueous solution of supporting electrolyte (0.5 M Na_2SO_4) was placed in the cell and flushed with argon. The solution was generally at acid pH and was titrated with base to raise the pH. At various points in the titration, weak base or salts of weak acids were used to achieve intermediate buffered systems. Strong base was used to obtain pH >10. A pH electrode (Fisher combination microelectrode) was used to continuously monitor the ph. Calibration of this electrode with standard buffers showed the recorded values to be within ±0.2 pH units of the buffered values.

Dark current-potential curves, capacitance data, and photocurrent data were determined as a function of pH for an electrode in supporting electrolyte only. The experiments were repeated with the addition of a particular ruthenium complex (10^{-5}-10^{-3} M). The magnitude of the photocurrent was determined as a function of excitation wavelength, ruthenium complex concentration, and incident light intensity.

Results

The presence of the polypyridineruthenium(II) complexes decreased the photocurrent produced by light of greater than band-gap energy and increased the photocurrent for light with sub-band-gap energy. The first effect is due to absorption of light by the ruthenium(II) complexes allowing less short-wavelength light to reach the electrode. In the second case the excited ruthenium(II) molecules produced by the long wavelength light are capable of electron donation to the TiO_2 thereby increasing the photocurrent. The photocurrents are

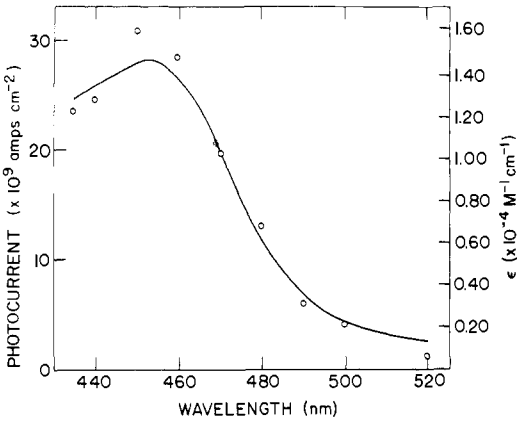

Figure 4. Comparison of the wavelength dependence of the $Ru(bpy)_3^{2+}$ sensitized photocurrent in TiO_2 with the absorption spectrum of $Ru(bpy)_3^{2+}$: photocurrent (O), absorption spectrum (full curve). The TiO_2 electrode was potentiostated at +0.50 V vs. SCE in 0.5 M H_2SO_4; $[Ru(bpy)_3^{2+}] = 9.4 \times 10^{-4}$ M.

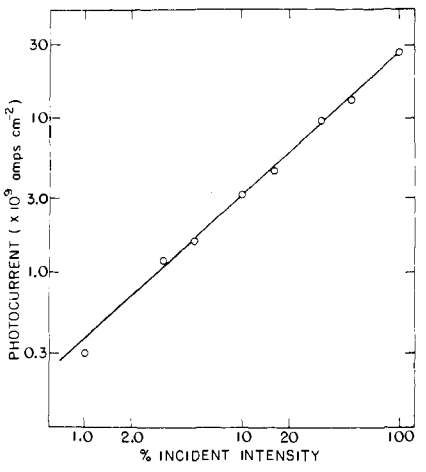

Figure 5. Light intensity dependence of the $Ru(bpy)_3^{2+}$ sensitized photocurrent in TiO_2: excitation wavelength is 460 nm with a 10 nm dispersion; 100% I_0 corresponds to an incident intensity of 1.03×10^{-7} einsteins cm^{-2} s^{-1}. The TiO_2 electrode was potentiostated at +0.50 V vs. SCE in 0.5 M H_2SO_4; $[Ru(bpy)_3^{2+}] = 9.4 \times 10^{-4}$ M.

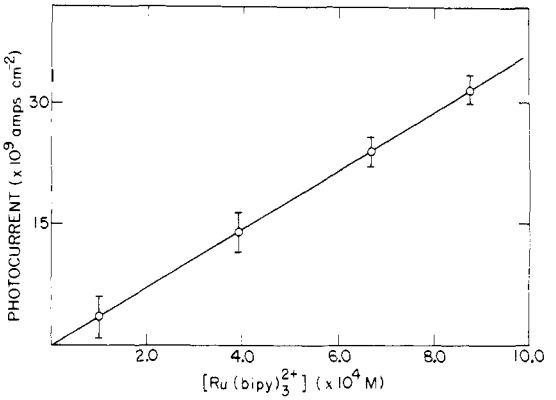

Figure 6. Variation of photocurrent with $[Ru(bpy)_3^{2+}]$: excitation wavelength is 460 nm with 10 nm dispersion. The TiO_2 electrode was potentiostated at +0.50 V vs. SCE in 0.5 M H_2SO_4. The error bars represent the uncertainty due to the noise level.

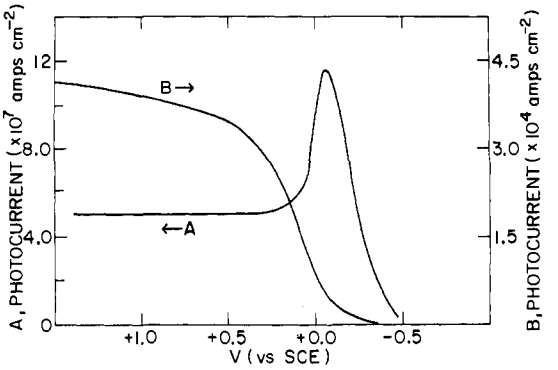

Figure 7. Photocurrent-potential curves for broad-band illumination of a TiO_2 electrode in 0.5 M H_2SO_4 containing $Ru(bpy)_3^{2+}$: curve A, visible illumination with Corning filters 5031 and 3389; curve B, band-gap illumination with Corning filter 5031. $[Ru(bpy)_3^{2+}] = 5.2 \times 10^{-4}$ M.

anodic as determined from the direction of the current flow in the ammeter. The wavelength dependence of the long-wavelength photocurrent is shown in Figure 4. As is evident from this figure the action spectrum, which is corrected for the xenon lamp output and solution absorption, corresponds rather closely to the absorption spectrum of the ruthenium complex. (A sharp rise of photocurrent at the shorter wavelengths, not shown, marks the beginning of photocurrent due to the band-gap excitation in TiO_2.) The photocurrent resulting from the excitation of the ruthenium(II) complex is directly proportional to the incident light intensity (Figure 5) and the ruthenium(II) concentration (Figure 6) under the conditions used.

Figure 7 depicts the photocurrent-potential curves at the TiO_2 electrode for wavelength regions covering band-gap and less than band-gap energies in the presence of the ruthenium complexes. (In the absence of ruthenium compounds, the equivalent photocurrents for curve A are only about 10% of those depicted and are about 10% higher for curve B.) All of the photocurrents level off at sufficiently positive potentials. Increasing the pH in the absence of the ruthenium complexes shifted the photocurrent-potential curves toward more negative potentials. The magnitude of the plateau photocurrents at sufficiently positive potentials (>+0.5 V) remained unchanged for both regions of light energies. By contrast, the photocurrents resulting from less than band-gap excitation of the ruthenium(II) complexes decreased significantly with increasing pH. The pH dependence of the plateau photocurrent at positive potentials is shown in Figure 8 and is discussed later.

Two methods were used to determine the flat-band potentials of the TiO_2 electrode. The first method involved the usual measurement of the space-charge capacitance C as a function of the applied potential V. The value of the flat-band potential V_{fb} was then obtained from the intercept of the plot of $1/C^2$ vs. V according to the Mott-Schottky equation (eq 1).[19]

$$\left(\frac{1}{C}\right)^2 = \frac{2}{\epsilon\epsilon_0 e_0 n_D}\left(V - V_{fb} - \frac{kT}{e_0}\right) \quad (1)$$

In this equation ϵ is the dielectric constant of the semiconductor (relative to a vacuum), ϵ_0 is the permittivity of free space, n_D is the donor density, and e_0 is the absolute value of the charge of the electron. Such a plot is shown in Figure 9. As is evident from this figure the intercepts of these plots are frequency dependent and can therefore not be used in assigning a value for V_{fb}. (This phenomenon has been recently treated in a series of papers.)[20-22] The slopes of the Mott-Schottky plots show little frequency dependence and a value of n_D can, therefore, be calculated from these plots. Using $\epsilon = 173$[13] the slopes of the Mott-Schottky plots give $n_D \sim 10^{19}$ cm^{-3} for the TiO_2 samples used in this work (values ranged from 0.8 to 2.2×10^{19} cm^{-3}).

A more reliable method[10b] of obtaining the flat-band potentials is to determine the potential at which the onset of

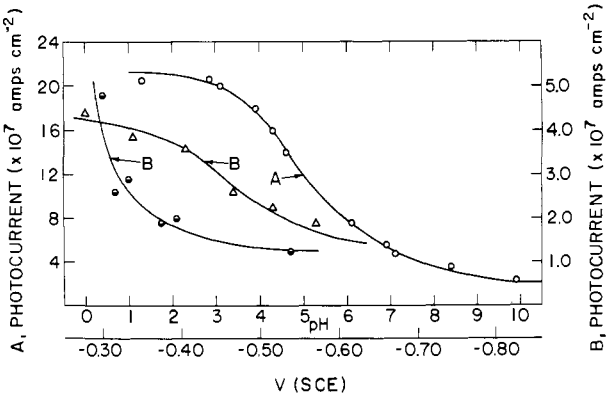

Figure 8. Spectrally sensitized photocurrents in TiO_2 vs. pH for the polypyridineruthenium(II) complexes: $Ru[4,7(CH_3)_2phen]_3Cl_2$ (○), $Ru(bpy)_3Cl_2$ (△), and $Ru[5\text{-}Cl(phen)]_3Cl_2$ (◒). The TiO_2 electrode was potentiostated at +1.0 V vs. SCE. Broad-band illumination using Corning filters 5031 and 3389. Bottom abscissa lists V_{fb} for TiO_2 at the various pH values (taken from Figure 10).

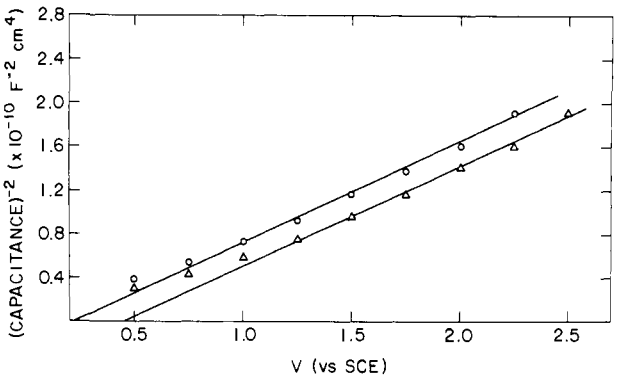

Figure 9. A Mott-Schottky plot of $1/C^2$ vs. potential for TiO_2 in 0.5 M H_2SO_4 at different frequencies for the AC excitation: 10 Hz (○), 100 Hz (△).

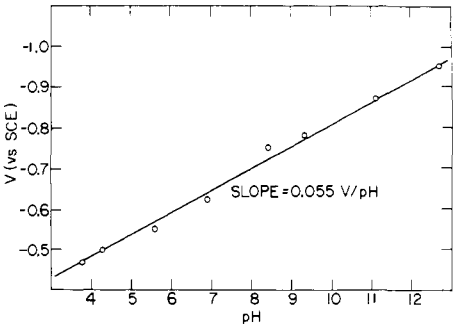

Figure 10. Potential for the onset of band-gap photocurrent vs. pH for TiO_2. Broad-band illumination with a Corning 5063 filter.

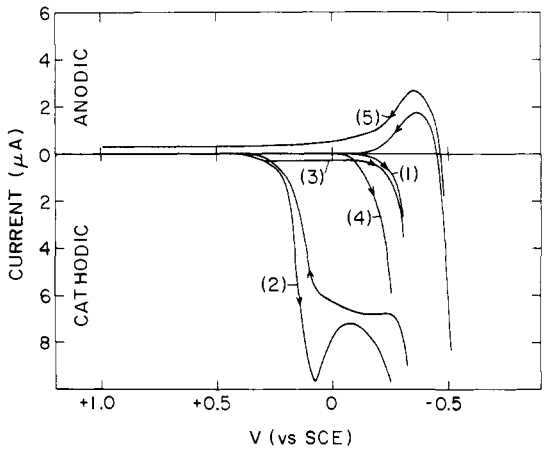

Figure 11. Current-potential curves for a series of redox couples at TiO_2 in 0.5 M H_2SO_4: (1) no added solute; (2) $Ru(bpy)_3^{3+}$, 10^{-3} M; (3) oxygen produced by band-gap illumination of TiO_2; (4) $Ru(H_2O)_6^{3+}$, 10^{-3} M; (5) Cr^{2+}, 8.0×10^{-3} M. Electrode area is 0.0821 cm^2; scan rate is 50 mV/s. Arrows indicate scan direction. Decrease in oxidizing power is $Ru(bpy)_3^{3+} > O_2 > Ru(H_2O)_6^{3+} > H^+ > Cr^{3+}$.

photocurrent occurs when the semiconductor electrode is illuminated by light with energy greater than or equal to the band gap of the semiconductor. The potentials determined in this manner are plotted as a function of pH in Figure 10. Over the pH range studied the flat-band potentials (vs. SCE) are given by eq 2.

$$V_{fb} = -0.25 - 0.055\ pH \qquad (2)$$

The slope of 0.055 V per pH unit is consistent with the slopes of similar plots for TiO_2[22] and other semiconductors[12,19] and has been attributed to the establishment of a protonic equilibrium at the electrode surface. The values of V_{fb} show generally good agreement with previously reported values.[22]

In order to further characterize the TiO_2 electrode dark cyclic voltammograms (sweep rate 20–50 mV/s) of a series of progressively weaker oxidizing agents (stronger reducing agents) were determined in 0.5 M H_2SO_4. The results show (Figure 11) that $Ru(bpy)_3^{3+}$ and O_2 are reduced about 0.5 V positive of V_{fb} while reduction of $Ru(H_2O)_6^{3+}$ and H^+ starts at about V_{fb}. In these cases no anodic current due to the oxidation of the reduced form of the couple was observed. Only with $Cr(H_2O)_6^{2+}$ was an anodic current obtained.

Discussion

The flat-band potential (vs. SCE) is the position of the Fermi level in the semiconductor when the energies of the bands for the semiconductor bulk and surface are equal. The position of the conduction band edge E_c^s (that is, the energy of the bottom of the conduction band at the semiconductor surface) can be related to the flat-band potential by eq 3[23,24b]

$$E_c^s = E_{F,fb} - kT \ln (n_D/N_c) \qquad (3)$$

where $E_{F,fb} = -e_0 V_{fb}$ and N_c is the effective density of states at the bottom of the conduction band. Substitution of $n_D = 10^{19}$ cm^{-3} and $N_c = 10^{20}$ cm^{-3} in eq 3 indicates that E_c^s lies only about 0.06 eV above $E_{F,fb}$.[24]

The relationship between E_c^s and the reduction potentials of the ruthenium complexes based on this work is shown in Figure 12. The E_c^s values[25] are the intercepts on the energy ordinate; to the left of this ordinate is depicted the energy of the bottom of the conduction band as a function of distance from the electrode surface for different values of the pH and applied voltage (bracketed values). (The band bending which occurs across the space-charge layer in the semiconductor is a consequence of the positive potential applied to the electrode.) To the right of the energy ordinate are shown the reduction potentials of the ground state and excited state ruthenium couples.[7]

Electron transfer at an electrode surface can be regarded as an isoenergetic process involving occupied and unoccupied states where the electrons move from the occupied to the unoccupied levels.[12] The rate of electron transfer to the electrode will therefore depend on the overlap of the occupied states of the excited ruthenium(II) complex with the unoccupied states in the conduction band of TiO_2. The magnitude of the anodic current is given by eq 4

$$I = k_c c_{red} \int_{E_c^s}^{0} \kappa(E) D(E) W_{red}(E)\, dE \qquad (4)$$

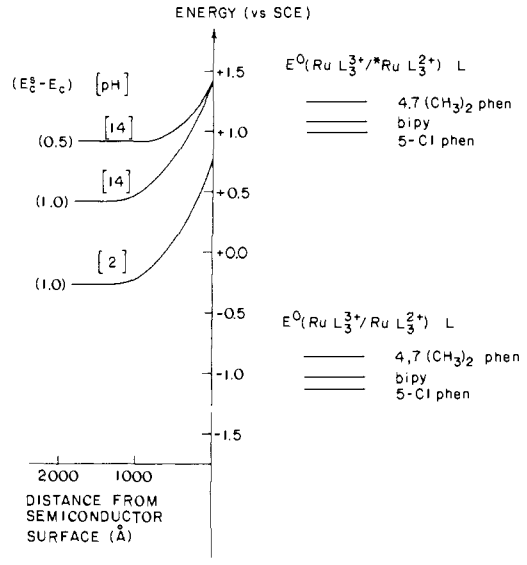

Figure 12. Energy levels in TiO_2 and polypyridineruthenium(II) complexes. The left of the diagram shows the change of the energy of the bottom of the conduction band as a function of pH and distance from the electrode surface for different applied positive potentials. The right-hand portion of the diagram shows the energies (E^0) corresponding to the standard reduction potentials (V^0) for the compounds listed in Table I and their lowest excited states ($E^0 = -eV^0$).[23] Distance from the electrode surface was calculated from eq 6 of ref 29.

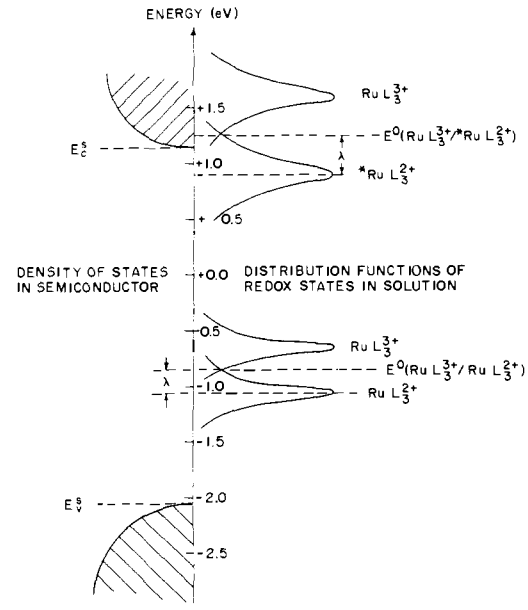

Figure 13. Density of states functions for TiO_2 and the distribution of energy states for the ground and excited state couples of a polypyridineruthenium(II) complex. The diagram is for the 4,7-$(CH_3)_2$phen derivative at pH 8. At first sight, the appearance of a distribution curve for RuL_3^{3+} in two different energy ranges is confusing. However, it must be remembered that one is dealing with two different redox couples. Also, λ is a quantity pertinent to a pair of ions and not to only a single species. Therefore λ as well as E^0 will differ for the two couples.

where k_c is the rate constant for electron transfer to the electrode, c_{red} is the concentration of the reduced form of the couple, $D(E)$ is the density of unoccupied states of energy E in the semiconductor, and $W_{red}(E)$ is the distribution function for finding the reduced form in a particular solvation state of energy E.

The density of the energy states in the semiconductor is large for energies greater than E_c^s and increases with the square root of the energy. For a harmonic oscillator model the solution distribution function $W_{red}(E)$ is given by eq 5[4,12,26]

$$W_{red}(E) = \exp[-\lambda(1 + (E - E^0)/\lambda)^2/4kT] \quad (5a)$$

$$= \exp[-(E - E^0 + \lambda)^2/4\lambda kT] \quad (5b)$$

where λ, the reorganization parameter, is the energy required to change the environment of the reduced form to that which would exist around the oxidized form at equilibrium, and E^0 is the energy corresponding to the standard reduction potential of the redox couple in solution ($E^0 = -e_0V^0$).[23] The distribution function for the oxidized form of the couple is similarly defined (eq 6).

$$W_{ox}(E) = \exp[-(E - E^0 - \lambda)^2/4\lambda kT] \quad (6)$$

The distribution functions for the reduced and oxidized forms have maxima at $(E^0 - \lambda)$ and $(E^0 + \lambda)$, respectively, and intersect at $E = E^0$. (By analogy with the semiconductor, $W_{red}(E)$ and $W_{ox}(E)$ can be regarded as the distribution function of occupied and unoccupied electron states of the redox couple.)

The value of the reorganization parameter can be estimated from the homogeneous exchange rates of the ruthenium complexes using the Marcus[26] relation $\lambda_{el} \approx \lambda_{homo}/2$. For the excited state ruthenium couple (eq 7)

$$^*Ru(bpy)_3^{2+} + Ru(bpy)_3^{3+} \rightleftharpoons Ru(bpy)_3^{3+} + {}^*Ru(bpy)_3^{2+} \quad (7)$$

$$Ru(bpy)_3^{2+} + Ru(bpy)_3^{3+} \rightleftharpoons Ru(bpy)_3^{3+} + Ru(bpy)_3^{2+} \quad (8)$$

$\lambda_{homo} \lesssim 0.7$ eV so that $\lambda_{el} \lesssim 0.35$ eV.[27] For the ground state couple (eq 8) λ_{homo} and λ_{el} are ~0.4 and ~0.2 eV, respectively. Because of the small λ values, the distribution functions for the ruthenium complexes are relatively narrow (Figure 13).

The relative positions of the distribution function of the excited ruthenium complex and the conduction band edge of TiO_2 define three photocurrent-potential regions. When $(E^0 - 2\lambda) > E_c^s$, the maximum anodic photocurrents can be observed. (In order to observe the maximum anodic photocurrent, an n-type semiconductor must be under at least a slight positive bias in order to efficiently collect all the injected electrons; when this bias becomes sufficiently positive all the injected electrons will be collected and the photocurrent will plateau (Figure 7).) Under zero or negative bias the semiconductor becomes degenerate and exhibits metal-like properties. Under these conditions the photocurrent will drop to zero. (Sensitized photocurrents are negligible at metal electrodes.)[3] When $(E^0 - 2\lambda) \lesssim E_c^s$, the photocurrents will begin to decrease as E^0 decreases or E_c^s increases and in the absence of tunneling effects (which are expected to be negligible for TiO_2)[14] the photocurrent will approach zero when $E^0 \approx E_c^s$. Figure 13 shows the top of the valence band is too low in energy (and has too few free charge carriers) to make any contribution to electron-transfer processes involving either ground or excited state ruthenium couples.

At low pH values there should be appreciable overlap between the occupied levels in the excited ruthenium(II) complex and the unoccupied levels in the conduction band of the TiO_2. Under these conditions the maximum anodic photocurrents are expected and observed (Figure 8). as the pH is increased (i.e., as E_c^s is increased), the amount of overlap between the excited ruthenium(II) levels and the unoccupied electrode levels diminishes and the photocurrents start to fall. As is expected from eq 4 and 5, the pH at which this fall-off begins shifts to higher values as the reduction potential of the excited state couple becomes more negative. The pH range over which the fall-off occurs should also reflect the width of W_{red}, i.e., the value of λ. The curve for the 4,7$(CH_3)_2$phen derivative is the most well-defined in this respect and exhibits a fall-off over a

0.4–0.5-V range ($2\lambda \lesssim 0.5$ eV). This range is consistent with the $\lambda \lesssim 0.35$ eV value used earlier. In this respect the data are at least qualitatively consistent with eq 4 and 5.

The above model also predicts that the photocurrent should decrease to half of its maximum value when $E_c^s \approx (E^0 - \lambda)$. This condition obtains at about −1.0 and −0.85 V (vs. SCE) for the 4,7(CH_3)$_2$phen and bpy complexes, respectively. In Figure 8, the pH values at which the photocurrents have decreased to half their maximum values implicate an E_c^s value which is about 0.4 eV larger than $E_{F,fb}$ and not, as eq 3 indicated, only 0.06 eV. This discrepancy might arise from errors in the calculation of the energy levels in the solution and/or the electrode. So far as the ruthenium complexes are concerned, the error in the excited state potentials is unlikely to exceed 0.1 eV. For the TiO_2 electrode, possible shifts in E_c^s could result from potential drops across the Helmholtz layer and/or from solute adsorption. In the usual model for the semiconductor–electrolyte interface it is assumed that the applied voltage is dropped entirely across the space-charge region of the semiconductor. This assumption[4,12] is based on the premise that the capacitance of the space-charge layer is much less than that of the Helmholtz layer. A recent article[22] showed that under conditions similar to those encountered here, a drop of <0.3 V can be anticipated in the Helmholtz layer. However, this change is in the wrong direction to account for the observed effect. Also, plots of the photocurrent at different applied biases as a function of pH show only minor differences in the curve profiles. Therefore, contributions from potential changes across the Helmholtz layer are ruled out. The most likely source for the discrepancy appears, therefore, to lie in the estimate of the value of N_c used in the earlier calculatio of E_c^s.

Adsorption of solute species also seems to play no part. The potential for the onset of band-gap photocurrent at any excitation wavelength was the same in the absence and presence of $Ru(bpy)_3^{2+}$ (Figure 7). The same result was obtained when $Ru(bpy)_3^{3+}$ was added; the sensitized photocurrent–pH curve determined in the presence of $Ru(bpy)_3^{3+}$ was the same as in its absence. In addition, as mentioned earlier, the sensitized photocurrent is proportional to the concentration of $Ru(bpy)_3^{2+}$ (up to 10^{-3} M).

The onset of $Ru(bpy)_3^{3+}$ reduction at voltages considerably positive of the values at platinum as well as no dark oxidation of $Ru(bpy)_3^{2+}$ was previously observed at TiO_2 in acetonitrile.[23] The experiment was repeated in this laboratory and essentially the same results were observed although the cathodic peak for $Ru(bpy)_3^{3+}$ was shifted to slightly less positive potentials. A peak indicating $Ru(bpy)_3^{3+}$ reduction could be observed in some cases when only $Ru(bpy)_3^{2+}$ was initially present in the solution. This occurred when the greater-than-band-gap excitation (wavelengths < 420 nm) was shut-off at a potential of +0.7 V vs. SCE when scanning in a negative direction. Sufficient $Ru(bpy)_3^{3+}$ was still present from $Ru(bpy)_3^{2+}$ oxidation by the holes produced in the valence band while the light had been on to give rise to the cathodic current. This was observed for both aqueous and acetonitrile solutions. The effect of $Ru(bpy)_3^{3+}$ reduction is also evident in the photocurrent–potential curves of Figure 7. At about the potential that $Ru(bpy)_3^{3+}$ reduction begins the photocurrent starts to increase and then peaks. Since $Ru(bpy)_3^{3+}$ can quench excited $Ru(bpy)_3^{2+}$, its reduction effectively increases the amount of $*Ru(bpy)_3^{2+}$ present at the electrode surface and this results in increased photocurrents.

These observations require a slight addition to the electron-transfer model and can be ascribed to the presence of an intermediate level (surface state) capable of carrying out reductions but not oxidations.[23] This interpretation is borne out in this work by the absence of anodic currents due to the oxidation of the reduced forms of $Ru(H_2O)_6^{3+}$ and H^+ (Figure 11). The potentials of these couples[28] lie at negative values with respect to the potential where $Ru(bpy)_3^{3+}$ reduction begins on TiO_2 but positive of V_{fb}.

In acetonitrile the energy of the intermediate level for TiO_2 is located 1.2 eV below the conduction band edge.[23] If the onset of $Ru(bpy)_3^{3+}$ reduction in an aqueous medium is taken as the energy of this intermediate level (+0.4 V vs. SCE in 0.5 M H_2SO_4), and if it is assumed that the difference between the energy of this level and E_c^s is the same in 0.5 M H_2SO_4 as it is in acetonitrile, then E_c^s is estimated to lie at +0.8 eV in 0.5 M H_2SO_4. This suggests a rather large difference (0.55 eV) between $E_{F,fb}$ and E_c^s. This estimate for E_c^s cannot be correct, however, in view of the fact that Cr^{2+} can be oxidized at TiO_2 in 0.5 M H_2SO_4 (Figure 11). Since V^0 for the Cr^{2+}/Cr^{3+} couple is −0.65 V vs. SCE in 0.5 M H_2SO_4,[28b] the oxidation of Cr^{2+} requires that E_c^s lie below +0.65 eV. This estimate of E_c^s is still considerably above the $E_{F,fb}$ value of +0.25 eV in 0.5 M H_2SO_4. As discussed earlier, the photocurrent measurements suggest that E_c^s lies about 0.35 eV above the value estimated from eq 3. If E_c^s in 0.5 M H_2SO_4 is ~0.6 eV, if the uncertainty in estimating λ is about 0.1 eV, and if the difference between $E_{F,fb}$ and E_c^s is independent of pH, then the results of this study are essentially consistent with the model depicted in Figures 12 and 13. The presence of the intermediate surface state on TiO_2 considerably enhances our confidence in the proposed model by providing an additional check on the relative values of $E_{F,fb}$ and E_c^s and confirms that the earlier estimate of $(E_c^s - E_{F,fb}) \sim 0.35$ eV is reasonable.

According to the model depicted in Figures 12 and 13, an E_c^s value of about 0.6 eV in 0.5 M H_2SO_4 fits in very well with the solute distribution curves and their photocurrent–pH profiles as it shows that the 5-Cl(phen) derivative should not exhibit a plateau region. It also shows that at pH 7, E_c^s is isoenergetic with a point well on the downward slope of the distribution curve for the reduced 4,7(CH_3)$_2$phen derivative as is required by the large photocurrents. Correspondingly, at acid pH the overlap of the levels for the 4,7(CH_3)$_2$phen derivative with the conduction band levels of TiO_2 should be quite extensive. As a result the quantum yield for electron injection should be close to unity. This quantum yield can be calculated by assuming that only those molecules that can diffuse to the electrode during the lifetime τ of the excited state can transfer an electron to the conduction band. As $\tau = 1.74$ μs,[7] the effective diffusion distance r is about 590 Å [$r = (2D\tau)^{1/2}$ where $D = 10^{-5}$ cm^2 s^{-1}]. Irradiation at the absorption peak maximum (445 nm) produces a flux of excited states of 2.16×10^{-8} mol cm^{-3} s^{-1}. With an effective volume element of 590×10^{-8} cm^3, the maximum current should be 1.3×10^{-8} A. The observed current is 1.2×10^{-8} A cm^{-2} and thus the quantum yield for electron injection is as expected essentially unity.

Implications for a Solar Energy Storage System. A previous report[16a] proposed the use of an electrochemical cell to effect the photodecomposition of water using visible light. This cell consisted of an n-type semiconductor connected to a platinum electrode in a pH 9 buffer containing $Ru(bpy)_3^{2+}$. The advantages and limitations of such a cell were discussed but no quantitative data were presented. The present studies show that the quantum efficiency for the photoinjection of an electron by an excited ruthenium complex can be very high and provide information on the energetic relationships that need to obtain between the ruthenium complex and the semiconductor electrode.

The quantum efficiency for the formation of hydrogen by $Ru(bpy)_3^{2+}$ sensitization of TiO_2 to 420–550 nm light in the above type of cell charged with 0.5 M H_2SO_4 is greater than 5% at 1 V bias. For a photoelectrochemical cell to function without any applied bias V_{fb} must lie negative of $V^0(H^+/H_2)$.[29] This condition, which must exist in order to produce a space-charge region in the semiconductor so that any pho-

toinjected electrons will be swept away from the surface and not recombine with the oxidized species in solution, is only marginally satisfied by TiO_2 (eq 2). Stable photoelectrode materials reported in the literature that satisfy this condition are $SrTiO_3$, $KTaO_3$, and $KTa_{0.77}Nb_{0.23}O_3$.[30,31] Their V_{fb} values are reported to lie 0.2 to 0.4 V more negative than that of TiO_2.[30,10b] However, if $(E_c^s - E_{F,fb})$ is the same for them as it is for TiO_2 (~0.35 eV) then at pH 9 (or even pH 1) E_c^s will lie at too high an energy for the ruthenium(II) complexes used in this work to be efficient sensitizers.[32] Only if $(E_c^s - E_{F,fb}) \leq 0.1$ eV will the overlap between the energy levels of the excited ruthenium complexes and those of the conduction band of the semiconductor be sufficient for photoinjection to occur. Choosing complexes with excited state levels lying at such high energies may require the use of light quanta of higher energy (which would decrease the response to sunlight) or the use of complexes with lower ground state reduction potentials (and therefore of lowered ability to oxidize water). Although these conditions are quite stringent they do not appear to be prohibitive and may well be satisfied by modifications of known polypyridine complexes.

References and Notes

(1) K. Hauffe, H. J. Danzmann, H. Pusch, J. Range, and H. Volz, *J. Electrochem. Soc.*, **117**, 993 (1970).
(2) H. Gerischer, *Photochem. Photobiol.*, **16**, 243 (1972), and references therein.
(3) R. Memming, *Photochem. Photobiol.*, **16**, 325 (1972), and references therein.
(4) H. Tributsch and M. Calvin, *Photochem. Photobiol.*, **14**, 95 (1971).
(5) M. Gleria and R. Memming, *Z. Phys. Chem. (Frankfurt am Main)*, **98**, 303 (1975).
(6) The energy difference between the lowest electronically excited level of $Ru(bpy)_3^{2+}$ and the bottom of the conduction band of SnO_2 is estimated from Figure 3 of ref 5. However, this value is somewhat in error as the energy scale is referenced to the standard hydrogen electrode but the redox potential for $Ru(bpy)_3^{2+}$ is placed at a value based on the saturated calomel electrode scale. Correcting for this error lowers the $Ru(bpy)_3^{2+}$ energies by 0.24 eV but still leaves an energy of 0.7 eV favoring electron injection.
(7) C-T. Lin, W. Böttcher, M. Chou, C. Creutz, and N. Sutin, *J. Am. Chem. Soc.*, **98**, 6536 (1976).
(8) G. Navon and N. Sutin, *Inorg. Chem.*, **13**, 2159 (1974).
(9) M. Gleria and R. Memming, *J. Electroanal. Chem.*, **65**, 163 (1975).
(10) (a) M. S. Wrighton, D. S. Ginley, P. T. Wolczanski, A. B. Ellis, D. L. Morse, and A. Linz, *Proc. Natl. Acad. Sci. U.S.A.*, **72**, 1518 (1975); (b) J. M. Bolts and M. S. Wrighton, *J. Phys. Chem.*, **80**, 2641 (1976).
(11) A recent report by L. A. Harris and R. H. Wilson, *J. Electrochem. Soc.*, **123**, 1010 (1976), notes aging effects of TiO_2 in 1 N acid. However, these effects are for band-gap light and for illumination times much greater than those used is these experiments.
(12) H. Gerischer, "Physical Chemistry: An Advanced Treatise", Vol. 9A, H. Eyring, D. Henderson, and W. Jost, Ed., Academic Press, New York, N.Y., 1970, p 463.
(13) P. J. Boddy, *J. Electrochem. Soc.*, **115**, 199 (1968).
(14) R. Memming and F. Mollers, *Ber. Bunsenges. Phys. Chem.*, **76**, 475 (1972), show that the tunneling distance $\chi(E)$ depends on the square root of the dielectric constant, ϵ. The tunneling probability, $T(E)$, is then proportional to $\exp(-K\chi(E))$ where K involves other terms. As $\epsilon_{TiO_2} > 10\epsilon_{SnO_2}$, $T(E)$ will be significantly lower for TiO_2 than for SnO_2.
(15) R. H. Sprague and J. H. Keller, *Photogr. Sci. Eng.*, **14**, 401 (1970).
(16) (a) C. Creutz and N. Sutin, *Proc. Natl. Acad. Sci. U.S.A.*, **72**, 2858 (1975); (b) G. Sprintschnik, H. W. Sprintschnik, P. P. Kirsch, and D. G. Whitten, *J. Am. Chem. Soc.*, **98**, 2337 (1976).
(17) (a) P. J. Holmes, "The Electrochemistry of Semiconductors", P. J. Holmes, Ed., Academic Press, New York, N.Y., 1962, p 370. This is similar to the etchant cited in ref 23; (b) T. Osa and T. Kuwana, *J. Electroanal. Chem.*, **22**, 389 (1969).
(18) Princeton Applied Research, Model 179 digital coulometer manual, 1975.
(19) R. Memming and F. Mollers, *Ber. Bunsenges. Phys. Chem.*, **76**, 469 (1972).
(20) E. C. Dutoit, R. T. Van Meirhaeghe, F. Cardon, and W. P. Gomes, *Ber. Bunsenges. Phys. Chem.*, **79**, 1206 (1975).
(21) R. DeGryse, W. P. Gomes, F. Cardon, and J. Vennik, *J. Electrochem. Soc.*, **122**, 711 (1975).
(22) E. C. Dutoit, F. Cardon, and W. P. Gomes, *Ber. Bunsenges. Phys. Chem.*, **80**, 475 (1976).
(23) S. N. Frank and A. J. Bard, *J. Am. Chem. Soc.*, **97**, 7427 (1975).
(24) The value of N_c is given by the expression $N_c = 2.48 \times 10^{19}(m^*/m)^{3/2}$ at 298 °C,[24a] where m^* and m are the effective mass and the mass of the electron, respectively. Values for N_c of 10^{19} cm^{-3} (ref 24b) and 10^{20} cm^{-3} (ref 22) appear in the literature and the difference arises from values chosen for m^*/m. The 10^{20} cm^{-3} value is based on $m^* = 3\text{–}5m$[24c] but this value is for slightly reduced material.[24c] Another article[24d] for strongly reduced TiO_2 estimates $m^* = 25m$. Using this value $N_c = 3.1 \times 10^{21}$ cm^{-3}, and with a donor density $n_D = 10^{19}$ cm^{-3}, one estimates that E_c^s lies about 0.15 eV above $E_{F,fb}$. (a) H. K. Henisch, "Rectifying Semi-conducting Contacts", Oxford University Press, London, 1955, p 43; (b) W. P. Gomes and F. Cardon, *Z. Phys. Chem. (Frankfurt am Main)*, **86**, 330 (1973); (c) G. A. Acket and J. Volger, *Physica (Utrecht)*, **80**, 1667 (1964); (d) H. P. R. Frederikse, *J. Appl. Phys.*, **32**, 2211 (1961).
(25) The values used for E_c^s in Figure 12 (and later in Figure 13) are those developed from arguments presented in ref 24 and in the remainder of this article, not those calculated from eq 3.
(26) R. A. Marcus, *J. Chem. Phys.*, **43**, 679 (1965).
(27) The reorganization parameter is calculated for ground state molecules and is assumed not to be significantly different for the excited state. This assumption is substantiated by solution quenching studies[7] of the excited state. For the case of an electrode reaction, $\lambda = 2\Delta G_{11}^{\ddagger}$.[26] The self-exchange rate constant k_{11} for the ground state $Ru(bpy)_3^{3+}/Ru(bpy)_3^{2+}$ couple is estimated as 2×10^9 M^{-1} s^{-1}, which gives $\Delta G_{11}^{\ddagger} = 2.4$ kcal mol^{-1}. For the excited state couple, $k_{11} \geq 10^8$ M^{-1} s^{-1} was selected,[7] which gives $\Delta G_{11}^{\ddagger} = 4.0$ kcal mol^{-1}.
(28) (a) R. R. Buckley and E. E. Mercer, *J. Phys. Chem.*, **70**, 3103 (1966); (b) W. M. Latimer, "Oxidation Potentials", 2nd ed, Prentice-Hall, Englewood Cliffs, N.J., 1952.
(29) H. Gerischer, *J. Electroanal. Chem.*, **58**, 263 (1975).
(30) (a) M. S. Wrighton, A. B. Ellis, P. T. Wolczanski, D. L. Morse, H. B. Abrahamson, and D. S. Ginley, *J. Am. Chem. Soc.*, **98**, 2774 (1976); (b) A. B. Ellis, S. W. Kaiser, and M. S. Wrighton, *J. Phys. Chem.*, **80**, 1325 (1976).
(31) J. G. Mavroides, J. A. Kapalas, and D. E. Kolesar, *Appl. Phys. Lett.*, **28**, 241 (1976).
(32) Preliminary experiments with single-crystal $SrTiO_3$ electrodes in 1 N H_2SO_4 show no sensitized photocurrents with $Ru(bpy)_3^{2+}$ and only minor photocurrents with the $4,7(CH_3)_2$phen derivative. SnO_2 thin film electrodes can be sensitized by $Ru(bpy)_3^{2+}$ in basic media.[5] However, its V_{fb}[9] lies about 0.4 V positive of $V^0(H^+/H_2)$ and thus the system must be biased in order to produce any sensitized photocurrent. Also, the very slow rise of photocurrent with applied potential (using band-gap light) indicates very inefficient carrier generation in SnO_2 thin film electrodes.